coatings

MDPI

Article

Effect of Coating Damage on the Micro Area Corrosion Performance of HDR Duplex Stainless Steel

Yufeng Lin, Zhuying Li *, Xiaoqiang Wang *, Xin Liu, Junhan Chi and Zhenhai Zhang

College of Naval Achitecture and Ocean Engineering, Naval University of Engineering, Wuhan 430033, China; lin18163558261@163.com (Y.L.); 18162626365@163.com (X.L.); cjh202401@163.com (J.C.); zzhzx305@126.com (Z.Z.)
* Correspondence: lzy18971394391@sohu.com (Z.L.); wxq_nue@126.com (X.W.)

Abstract: In order to determine the effect of damaged insulating enamel on the corrosion of high-chromium (H), duplex (D), and corrosion-resistant (R) duplex stainless steel, the corrosion characteristics of HDR duplex stainless steel in 3.5% NaCl solution were studied by means of local electrochemical impedance spectroscopy (LEIS) and micro-morphology analysis. It was shown that the LEIS impedance was stable at about 7.0 × 10^3 Ω within 10 days when the HDR duplex stainless steel was not coated. The minimum LEIS impedance of exposed HDR at the damaged area fluctuated around 6.5 × 10^3 Ω within 15 days when the coating of the self-control insulating enamel damaged area was 1 mm × 10 mm. The coating-damaged area from 1 mm × 10 mm reduced to a circular hole with a diameter of φ1 mm, and the LEIS impedance of the exposed HDR increased at the damaged coating. When extending along the damaged coating to the intact coating area, the impedance rapidly increased, and the further the distance from the damage, the greater the increase in impedance. The impedance of coated HDR increased with the prolongation of immersion time and ultimately stabilized. The thicker the coating, the longer the impedance took to reach a stable state. The stabilized coating had a better effect on improving the corrosion resistance of HDR duplex stainless steel. Within 15 days, the HDR ferrite structure at different areas of coating damage prioritized corrosion. Cl^- mainly comes from the solution, and Si and S elements mainly come from elements of the collective itself, with Cl^- adsorption, S, and Si element inclusion being the main factors influencing the corrosion of the ferrite structure.

Keywords: coating damaged; HDR duplex stainless steel; micro area corrosion; structure

check for updates

Citation: Lin, Y.; Li, Z.; Wang, X.; Liu, X.; Chi, J.; Zhang, Z. Effect of Coating Damage on the Micro Area Corrosion Performance of HDR Duplex Stainless Steel. *Coatings* **2024**, *14*, 174. https://doi.org/10.3390/coatings14020174

Received: 20 November 2023
Revised: 4 January 2024
Accepted: 10 January 2024
Published: 30 January 2024

Copyright: © 2024 by the authors. Licensee MDPI, Basel, Switzerland. This article is an open access article distributed under the terms and conditions of the Creative Commons Attribution (CC BY) license (https://creativecommons.org/licenses/by/4.0/).

1. Introduction

Duplex stainless steel is mainly composed of austenite (γ-phase) with a face-centered cubic structure and ferrite(α-phase) with a body-centered cubic structure. It has the characteristics of austenitic stainless steel and ferrite stainless steel, high yield strength, and fatigue strength, and it is also cost-effective and resistant to electrochemical corrosion and stress corrosion [1,2]. It has good application prospects in the petrochemical industry, ship pipeline, ocean engineering, etc. [3,4], but corrosion of duplex stainless steel is inevitable in the actual environment. At present, applying a corrosion-prevention coating is one of the most important methods that can be used to improve the corrosion resistance of stainless steel [5]. There must be conductive electron and ion currents in the cathode and anode regions when the metal is electrochemically corroded. The coating with good electrical insulation can inhibit the dissolution of anode metal ions and the discharge of the cathode in the solution. Therefore, the organic coating on the surface of the metal substrate can significantly block the ion movement between the anode or cathode and the solution, and the resistance of the coating can block the transmission of ions and slow the occurrence of corrosion.

HDR is low-carbon and high-chromium (H), duplex (D), and corrosion-resistant (R) duplex stainless steel as new corrosion-resistant steel. Corrosion phenomena, such as

seawater pipelines, flanged nipples, flange sealing surfaces, and welding place have also been found [6,7], and corrosion protection via coating has achieved a good protection effect. However, due to the long-term effects of human and mechanical stress and corrosive media, the coating inevitably exhibits phenomena such as peeling, breakage, and foaming [8,9]. At present, electrochemical impedance spectroscopy (EIS) is widely used to analyze the protection of coatings on metals [10–12], which evaluates the protective effect of coatings to a certain extent. However, coating failure and matrix metal corrosion often start in local areas, and EIS cannot obtain information related to local corrosion. Subsequently, methods represented by LEIS have been developed that can better characterize local corrosion. Gao Jin et al. studied the influence of seawater pressure on the protective performance of deep-sea epoxy coatings by means of LEIS [13].

Although LEIS obtained partial coating failure information, the matrix was entirely composed of metals that are prone to corrosion [14]. There is a lack of research on the change of substrate with good corrosion-resistant metals when the coating is damaged, and the plane test data and the line test data of LEIS have yet to be combined for analysis of the change characteristics of substrate corrosion, highlighting the lack of relevant research on the corrosion change of corrosion-resistant metals. Thus, it has yet to be determined whether coating protection has been applied, and further research is needed to evaluate the change of impedance in different regions with coatings damaged at the initial stage in the corrosion solution for stainless steel.

In order to grasp the differences in corrosion changes of the damaged substrate coatings compared with metals with good corrosion resistance—such as HDR double-phase stainless steel and common corrosive metals such as carbon steel—and evaluate the protective effect of self-made epoxy-insulating enamel on HDR corrosion after coating damage, this study uses self-made enamel as the coating, selects HDR double-phase stainless steel as the substrate, artificially controls the amount of coating damage, and studies the corrosion resistance of local coating damage using micro-electrochemical impedance spectroscopy (LEIS). The plane test data and line data of LEIS are fully mined, and the influence of coating damage on the HDR corrosion resistance is studied by combining microscopic observation and energy spectrum analysis, which provides a theoretical basis for further understanding the influence of coating damage on HDR corrosion resistance and subsequent corrosion-resistant metal coating protection.

1.1. Sample Preparation

The pipeline of HDR Duplex stainless steel with a diameter of 20 cm, thickness of 5 mm, and length of 1.5 cm was cut into 62 equal parts, and then 240# sandpaper was used to grind it into 1 cm × 1 cm samples. The axis surface (inner surface) of HDR specimens was taken as the research surface, and copper wires were welded on the back. Then, they were sealed with epoxy resin, exposing the working face of 1 cm × 1 cm. They were polished with sandpaper to 2000#. They were sonicated with deionized water, cleaned with acetone to remove oil stains, and dried. HDR duplex stainless steel components are shown in Table 1.

Table 1. Chemical composition of HDR duplex stainless steel.

Chemical Element	C	Mn	Si	S	P	Ni	Cr	Mo	N	Fe
Mass (%)	0.018	1.28	0.44	0.001	0.024	6.42	24.59	2.16	0.16	64.907

After sticking the cut 1 mm wide and Φ1 mm patterned paper on the polished sample surface, the self-made insulating enamel was brushed; then, the patterned paper was torn off immediately after brushing, leaving artificial damage in the form of holes. The sample was left to cure at room temperature for 15 days, and then the damaged samples with the artificial coating were prepared.

1.2. Electrochemical Tests and Structure Observation

Localized Electrochemical Impedance Spectroscopy (LEIS) was conducted on a Princeton system (model AMETEK, Berwyn, PA, USA) electrochemical workstation using the VersaSCAN software driver (https://www.ameteksi.com/). Experiments were carried out using a conventional electrode cell assembly with a saturated calomel electrode (SCE) as reference electrode (RE); all potentials were given with respect to the SCE, a platinum sheet served as the counter electrode, and HDR specimens were used as working electrodes. The step mode was used to test on the X-Y plane, and the test area was 12 mm × 12 mm, with a 200 μm interval between every two points, 1000 Hz frequency, relative open circuit potential of 0 mV, and 3.5% NaCl solution as the electrolyte. The test probe could be automatically returned to the initial setting point by the software used after the last measurement. The sample was soaked in the electrolytic pool for 15 days to keep still to ensure that the test distance between the probe and the sample surface was consistent each time. The samples were electrolytically etched in 30% KOH solution for 15 s, rinsed with deionized water, blown dry, and then observed with a 3D metallographic microscope (VHX-5000 Keyence, Shanghai, China). Electronic scanning electron microscope (SEM) (ZEISS, Model EVO10, Shanghai, China) was used to observe the surface tissue corrosion morphology, and energy-dispersive spectroscopy (EDS) (OXFORD Instruments, Oxford, UK) was performed using an energy dispersive spectrometer. The SEM test voltage was 15 kV.

2. Results and Analysis of Experiment

2.1. HDR Metallographic Morphology

Figure 1 shows the morphology and SEM of the HDR structure, showing that the dark structure was α phase (ferrite), marked by spectrum 1 in Figure 1b. The bright part is the γ phase (austenite), which is marked with spectrum 2 in Figure 1b. The inclusions were mainly spot-like and distributed in the ferrite structure and its boundary. The dual phase was alternately distributed, and the proportion of the structure area was similar. In the EDS analysis in Table 2, ferrite, Cr, and Mo content is high, as well as the austenitic Fe and Ni content. The austenite contains a higher content of Ni, about 6.9%, while the ferrite contains relatively less Ni, about 4.4% (as shown in Table 2), which is an important basis for the EDS analysis phase structure of α and γ as follows.

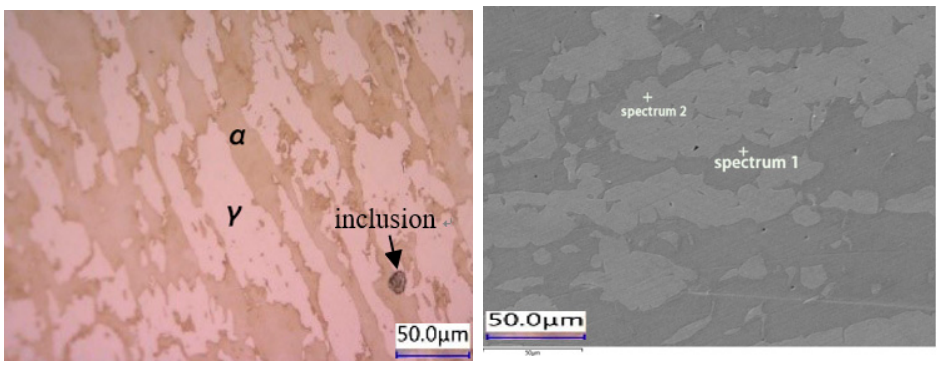

(**a**) (**b**)

Figure 1. Metallographic and SEM of HDR. (**a**) Metallographic of HDR. (**b**) SEM of HDR.

Table 2. Results of EDS with HDR duplex stainless steel (wt.%) marked in Figure 1a (mass %).

Sample	Structures	Marked	Fe	Cr	Ni	Mn	Mo	Si
HDR (%)	Austenite (γ)	Spectrum 1	64.0	27.6	4.4	1.3	2.7	
	Ferrite (α)	Spectrum 2	66.6	23.2	6.9	1.5	1.5	0.3

2.2. LEIS Test of HDR Uncoated

The LEIS technique used a bimetallic probe to measure the voltage drop in a local region of the solution. Applying an AC voltage would produce a corresponding AC current. The local current generated on the sample surface would also be different due to the local activity of the sample. Based on this principle, the surface impedance of the sample was tested [13]. Figure 2 shows the LEIS diagram of HDR duplex stainless steel without coating, where the edge of the resin sealing surface impedance is large, and the smaller part of the impedance in the middle is the impedance of the HDR-exposed matrix. It can be seen in Figure 2a that the lowest impedance on the first day is about 6.5 × 10^3 Ω, and Figure 2b shows that the lowest impedance on the second day was about 7 × 10^3 Ω. Figure 2c shows that the lowest impedance was still 7 × 10^3 Ω for 10 days, and this was related to the state of a passivation film on the surface of HDR. At the beginning of immersion in the 3.5% NaCl solution, passivation film quickly formed on the surface of HDR, but the passivation film was not very dense. However, with the extension of the soaking time, the oxygen in the solution was sufficient, and the surface of HDR continued to oxidize into film. Moreover, the passivation film becomes dense and stable after 2 days. The surface state of HDR hardly changed, and the impedance remained unchanged until the 10th day. Figure 2d shows the distribution of LEIS impedance data obtained by HDR at different times of 1st day, 2nd day, and 10th day when x = 6 mm in the middle of the sample, which could more intuitively show the change characteristics of LEIS impedance on the HDR surface. The particularly large impedance change at both ends is the epoxy resin sealing surface, and the middle section of the horizontal line impedance is HDR duplex stainless steel. The figure shows that the curve shape shifted to the right on the second day, which was mainly caused by the horizontal fine adjustment of the starting point of the LEIS probe during the test. It could also be seen that the LEIS test curves almost coincided with 10 days, indicating that the HDR impedance without exposed coating at x = 6 remained unchanged within 10 days, and the HDR surface state maintained good stability [14,15].

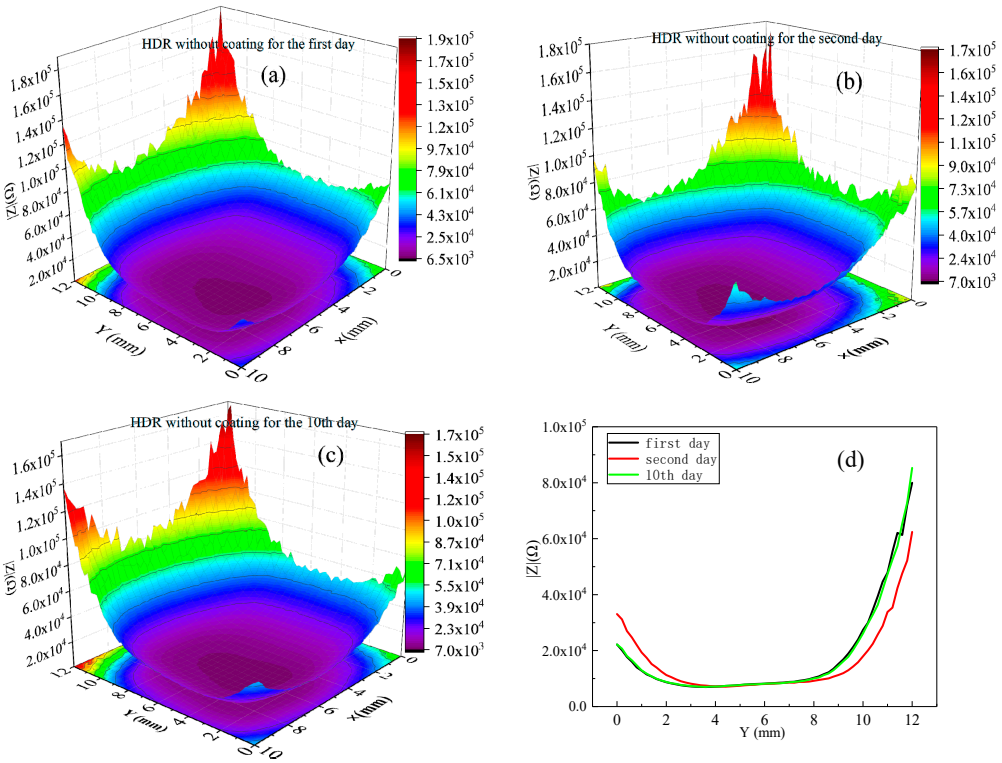

Figure 2. LEIS impedance of HDR duplex stainless steel without coating at different times. (**a**) LEIS for first day. (**b**) LEIS for 2nd day. (**c**) LEIS for 10th day. (**d**) LEIS at the middle position (× = 6 mm) of the HDR.

2.3. LEIS Test of HDR with Coating Damaged

The coating damage test was performed on a 10 mm × 10 mm specimen with the LEIS test area of 12 mm × 12 mm to ensure that all areas of the specimen surface can be tested. Figure 3a shows that there was a 1 mm × 10 mm strip of uncoated specimen in the middle and a well-coated area on both sides. Figure 3b shows the 3D surface morphology of the damaged coating sample, indicating that the coating thickness was 47.92 µm.

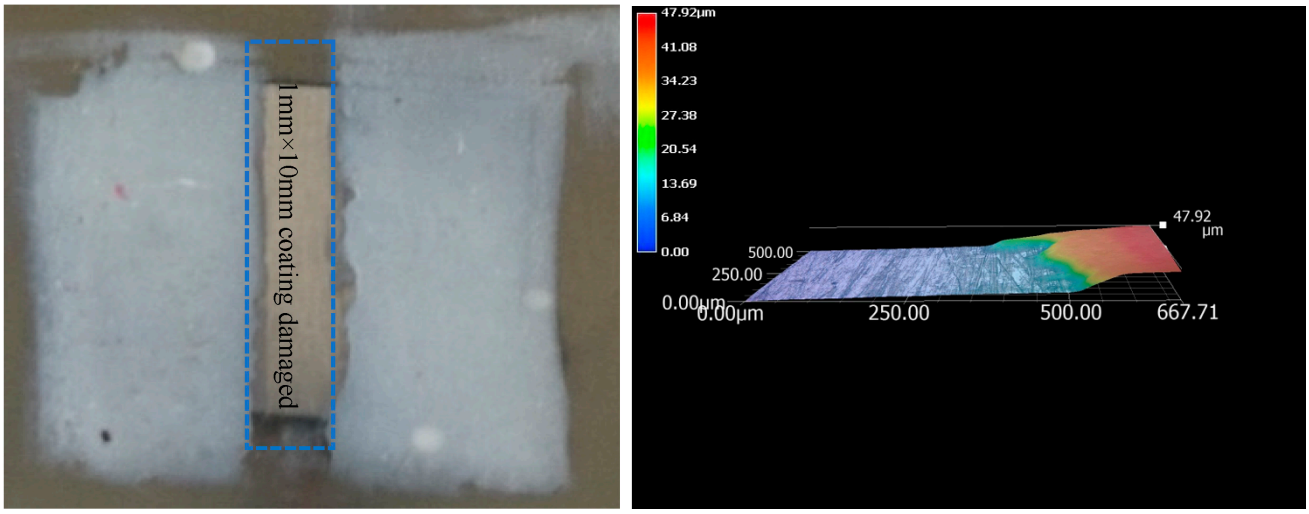

(**a**) (**b**)

Figure 3. Macro-morphology and 3D morphology of HDR with the 1 mm × 10 mm wide coating damaged in the middle. (**a**) The 1 mm × 10 mm wide damaged coating. (**b**) The 3D morphology of damaged coating diagram.

Figure 4 shows the corresponding LEIS impedance of the sample surface during 15 days of HDR immersion in 3.5% NaCl solution. Figure 4a shows that the lowest impedance at the 1 mm × 10 mm coating damaged on the first day was 6.45 × 10^3 Ω. Figure 4b showed that it rised to 8.5 × 10^3 Ω on the second day, Figure 4c show that it falled into 6.5 × 10^3 Ω at tenth day, and Figure 4d show that it reached 6.0 × 10^3 Ω at fifteenth day. Figure 4e shows the comparison of the test results of all the intermediate 1 mm × 10 mm coating damage tests after 15 days. The impedance of the bare substrate is shown as the blue part, and the impedance of the part protected by the coating at both ends is shown as the yellow or red part. It was found that the LEIS impedance of the whole sample was almost on a horizontal plane on the first day, while the LEIS impedance showed a "U" shape on the second day. The LEIS impedance of the blue part of the LEIS intermediate matrix within 15 days basically overlapped, and the impedance fluctuated around 6.5 × 10^3 Ω. On the whole, the impedance of the coated damaged part was not much different for the uncoated HDR sample during the soaking time, indicating that the corrosion resistance of the damaged part was comparable for the HDR sample, and the coatings on both sides had no effect on the impedance at the exposed HDR matrix in the middle. There was a big difference in the coated area; the impedance of the coated area on the second day was much greater than that on the first day, and the LEIS impedance of the coated surface from 2 days to 15 days was different from each other, but the difference was not large. The results showed that although the impedance of the whole surface of the sample with coating protection was higher than that without coating protection on the first day, the coating had a better protection effect on the HDR matrix, but the LEIS impedance with coating increased sharply after the second day, meaning the protection effect on the sample with coating was much better after two days in the 3.5% NaCl solution.

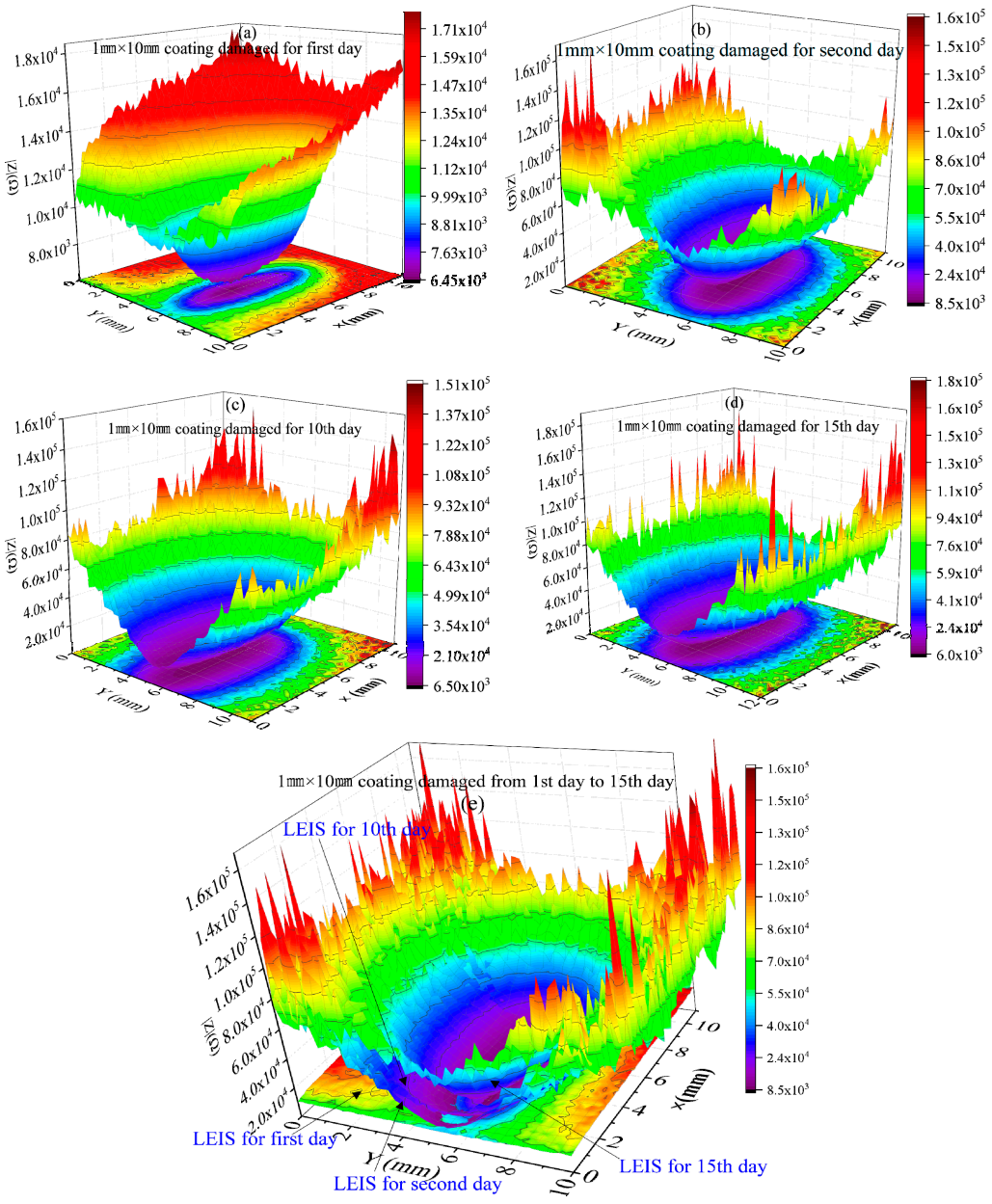

Figure 4. LEIS impedance of coating damaged with 1 mm × 10 mm strip in the middle at different times. (**a**) LEIS for first day. (**b**) LEIS for 2nd day. (**c**) LEIS for 10th day. (**d**) LEIS for 15th day. (**e**) LEIS from 1st day to 15th day.

Figure 5 shows the LEIS diagram of the middle 1 mm × 10 mm strip coating damaged at x = 6 mm in the middle of the sample at different times, which could more clearly reflect the variation trend of LEIS impedance on the surface of HDR samples at different times. Figure 5a shows that on the first day, the impedance at the coating damaged was the lowest, about 6.5 × 10^3 Ω, and the impedance increased gradually along the coating damaged to the protected coating on both sides until it reached the sealed edge of the sample, and the maximum impedance at the coated coating can reach 1.6 × 10^4 Ω. Figure 5b shows that the impedance at the damage site increased slightly on the second day, and the impedance at the coating site rose faster than that on the first day. The impedance distribution still gradually increased along the damage site to the protected area with the coating on both sides, and the further away from the damage site, the greater the increase in the impedance, up to 1.0 × 10^5 Ω, but with the continuous extension of soaking time, the impedance fluctuated. For the 1 mm × 10 mm damaged strip coating, the HDR matrix in the exposed

area not only accelerated corrosion but also maintained good corrosion resistance within 15 days, which was quite different from the corrosion characteristics of the metal easily corroded in the damaged area of the coating [16,17]. This may be related to the fact that HDR duplex stainless steel easily formed a dense passivation film in a sufficient oxygen solution [18], resulting in better corrosion resistance. At the same time, although dense passivation film formed on the surface of HDR duplex stainless steel, the resistance of HDR with the homemade coating was higher than that without coating protection, and the protective effect was better. However, due to the damage to the coating, the shielding performance at the edge was weakened, and the cations generated by HDR corrosion were easy to penetrate [19]. The closer it was to the coating, the stronger the diffusion ability of cations, and the closer it was to the coating damage, the more the protective effect was weakened. Moreover, with the extension of the soaking time, the impedance of the coated HDR matrix increased significantly on the second day and then remained stable, indicating that its corrosion resistance was further improved with passivation film formation.

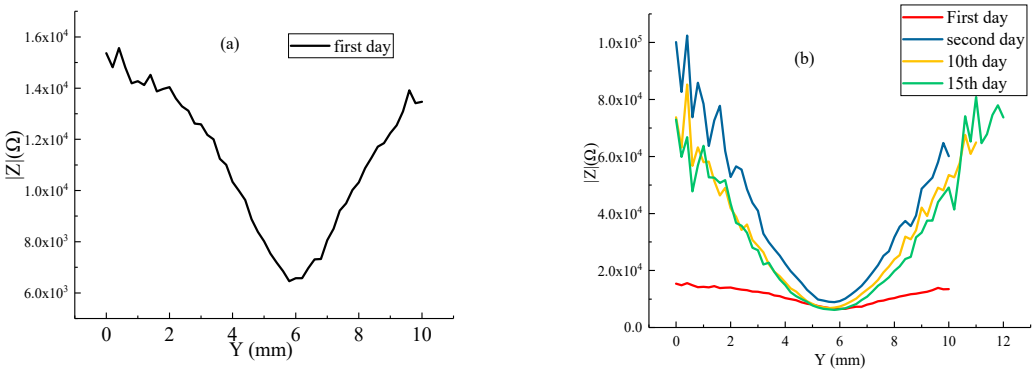

Figure 5. LEIS impedance of 1 mm × 10 mm strip coating damaged at the middle of × = 6 mm. (**a**) For 1 day. (**b**) From 1 day to 15 days.

As shown in Figure 6, the soaking HDR matrix 15 days after the 1 mm × 10 mm intermediate strip coating was damaged, a small amount of corrosion products appeared (as shown in the yellow mark), and the corrosion products were convex and spot-like. Since HDR duplex stainless steel was mainly composed of ferrite and austenite, and EDS analysis showed that the raised corrosion products marked with spectrogram 3 and the contain of Ni was 3.6% in Table 3, which was thought to be ferrite (structural analysis was performed in another article). The non-corroded areas were marked with spectrogram 4, where the content of Ni was 7.6%, and it was thought to be austenitic structures. This indicated that corrosion occurred first in the ferrite structures. Moreover, there was a greater content of Na, Cl, and S elements in the area of HDR corrosion products in Table 3 on the ferrite than in the matrix in Table 2. The elements Na and Cl were mainly derived from the corrosive medium, while S might be derived from inclusion components in the ferrite.

Table 3. The result of EDS for different areas marked in Figure 6 (mass %).

Marked	Fe	Cr	Ni	Mn	Mo	Si	S	Cl	Na
Spectrum 3	62.1	27.3	3.6	1.6		0.5	0.8	0.9	3.2
Spectrum 4	65.1	23.4	7.6	1.5	1.8	0.5			

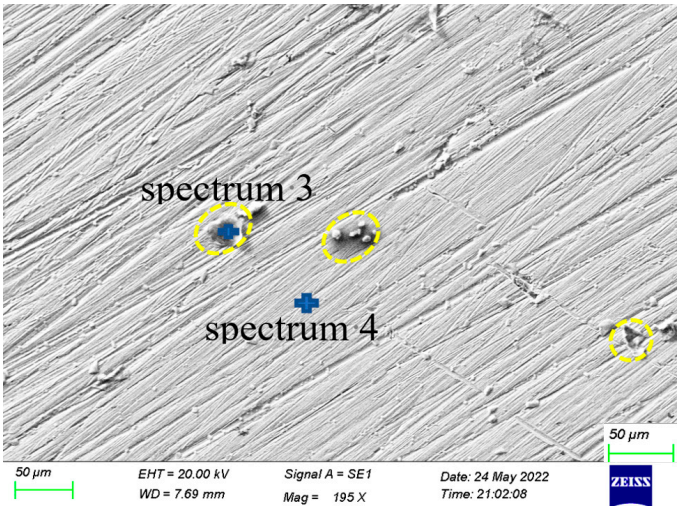

Figure 6. SEM of HDR matrix with 1 mm × 10 mm strip coating damaged in the middle.

Figure 7a shows that the HDR duplex stainless steel surface coating has two damaged coating holes with a diameter of φ1 mm at the middle and edge of the 10 mm × 10 mm sample. Figure 7b shows that the coating thickness with holes was 72.18 µm, which was thicker than the coating thickness of the damaged coating sample with a 1 mm × 10 mm strip.

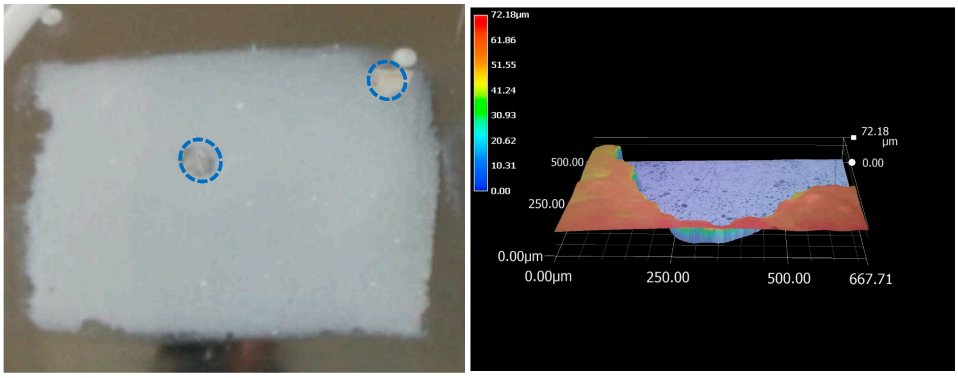

(**a**) (**b**)

Figure 7. Macro morphology and 3D morphology of HDR with diameter φ1 mm coating damage. (**a**) Diameter φ1 mm coating damage. (**b**) The 3D morphology of HDR with coating damage.

Figure 8 shows the LEIS diagram of various parts of the HDR surface with φ1 mm coating damaged at different times. Figure 8a–d shows that the lowest impedance at the coating damaged was 1.278 × 10^4 Ω on the 1st day, 1.248 × 10^4 Ω on the 2nd day, 1.90 × 10^4 Ω on the 10th day, and 2.2 × 10^4 Ω on the 15th day, respectively. The data showed that the difference in impedance at the lowest point of the entire sample surface was only 30 Ω between the 1st and 2nd days, while the impedance changed for the 10th day. There was a big difference from 10 days to 15 days, and the difference in impedance was over 3 × 10^3 Ω. Figure 8e shows the LEIS diagram at the middle of x = 6 mm in the middle of the sample on the first and second days (through the coating damage). It was found that the impedance increased gradually from the coating damage to the coating, and the further away from the coating damage, the greater the increase in amplitude. The maximum impedance could reach about 1.9 × 10^4 Ω, which also reflected that the coating had a good protective effect on HDR. Figure 8f shows the LEIS diagram at x = 6 mm in the middle of the sample within 15 days. At this time, the LEIS impedance of the φ1 mm coating damage sample for the first 2 days was almost a straight line, while the impedance was U-shaped after 10 days. The further away from the coating damage, the greater the impedance of

HDR increased. The maximum impedance after 10 days reached about 1.1 × 10^5 Ω, and the maximum impedance after 15 days was still 1.1 × 10^5 Ω, indicating that the impedance at the coating after 10 days was greatly improved, and the impedance under the coating reached stability on the 10th day. In the first 2 days, the minimum impedance of the HDR substrate exposed to φ1 mm coating damaged was barely increased, and the impedance of the coating was greater than that of the exposed sample. Even after 10 days, the minimum impedance of the substrate in the damaged, exposed area increased, and the impedance of the coated part increased much faster than the substrate without coating. The results showed that the impedance of coated HDR samples and coating damage increased with the extension of soaking in the first 15 days, but the impedance of coated HDR samples increased more significantly with the extension of soaking. The impedance after 10 days was much larger than that in the first 2 days, indicating that HDR corrosion resistance had a better protective effect when soaked in a solution for the first 15 days with coating damage.

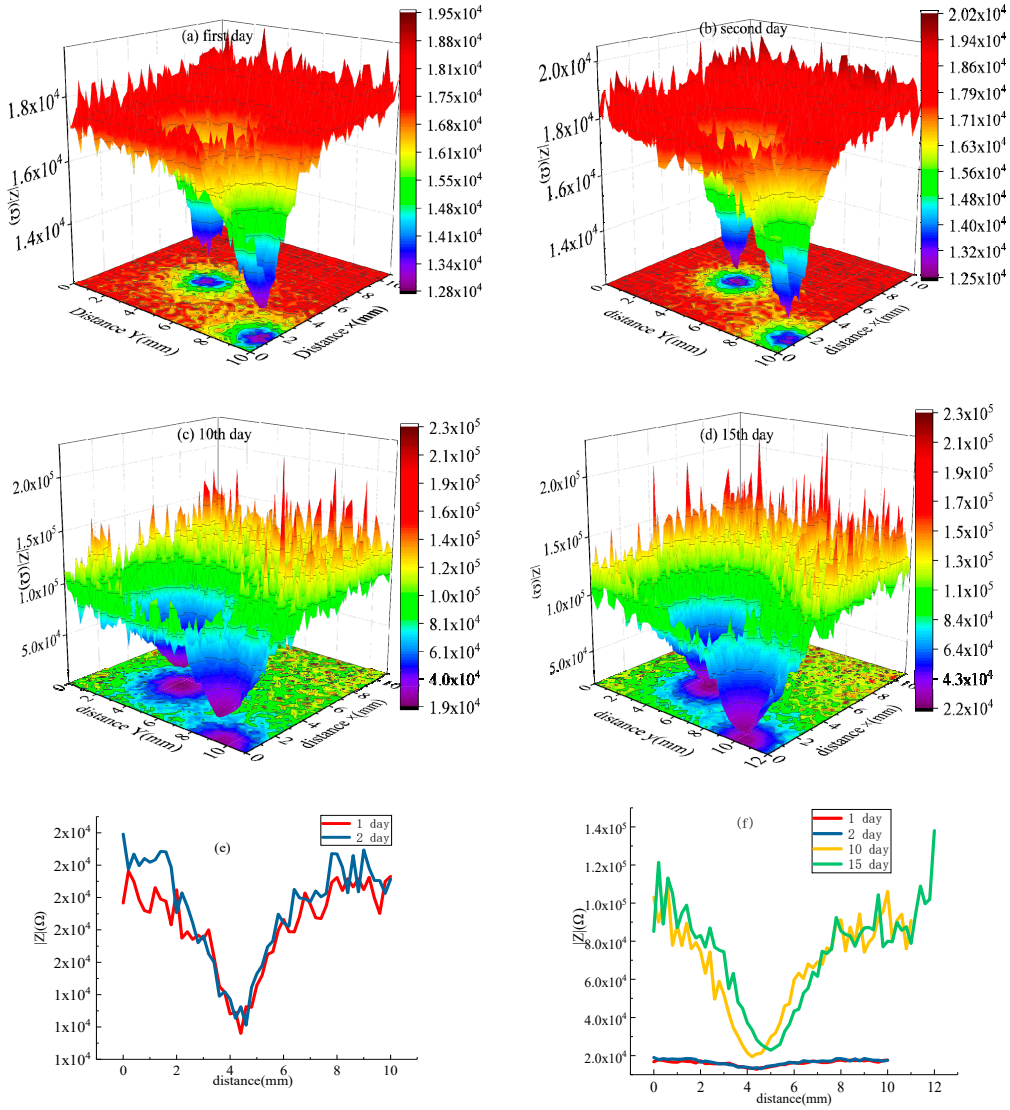

Figure 8. LEIS of HDR with φ1 mm damaged circular hole coating and the position of × = 6 mm at different times. (**a**) LEIS for first day. (**b**) LEIS for second day. (**c**) LEIS for 10th day. (**d**) LEIS for 15th day. (**e**) From 1 day to 2 days (× = 6 mm). (**f**) From 1 day to 15 days (× = 6 mm).

Figure 9 shows the SEM image and metallographic structure of the φ1 mm damaged round hole coating after 15 days. Figure 9a shows that pitting corrosion also occurred on the exposed HDR substrate after 15 days. According to EDS analysis, the corrosion spots are marked as spectrogram 5, and non-corroded spots are marked as spectrogram 6. As shown in Table 4, the corrosion point contains Ni 4.9%, while the non-corroded matrix contains Ni 8%. It is inferred that after the φ1 mm round hole coating is damaged, the ferrite structure is corroded first, and the corrosion point contains elements such as Cl, S and Si. Figure 9b shows the corrosion morphology of a metallographic structure after the φ1 mm round hole coating was damaged for 15 days. It was found that the pitting corrosion mainly occurs in the ferrite structure, which further confirms the speculation that corrosion occurs in ferrite first. After soaking for 15 days, as shown in Figure 9c, the coating is well combined with HDR, and there is no seam or peeling at the edge. Figure 9d is an enlarged image of the coating in Figure 9c. Due to the crosslinking reaction between the coatings caused by the addition of different components, there are some small holes scattered on the surface of the coatings, which are all less than 0.5 μm and distributed in the crosslinking substance with a white boundary. Although pores appeared in the coating during the crosslinking reaction, no corrosion was found on the substrate under any pores. Table 5 shows the results of EDS analysis of different areas of the coating in Figure 9d. Spectrum 7 shows that the coating is mainly composed of elements such as C, O, and Si, while the white part around the pores in the coating is shown in spectrum 8, which is mainly composed of C, O, and Si. The pores marked in spectrogram 9 contain elements such as C, O, Si, and Ti (among which Cl is the element involved in the corrosion solution). The marker in spectrogram 10 is white granules, which are mainly composed of elements such as C, O, and Ti. All the pores occur in the white granular substance, and the white granular substance has more Ti than the normal coating, so it is speculated that the pores are mainly generated by this substance and its vicinity because of the fast crosslinking reaction or the rapid precipitation of filler particles such as TiO_2 and mica.

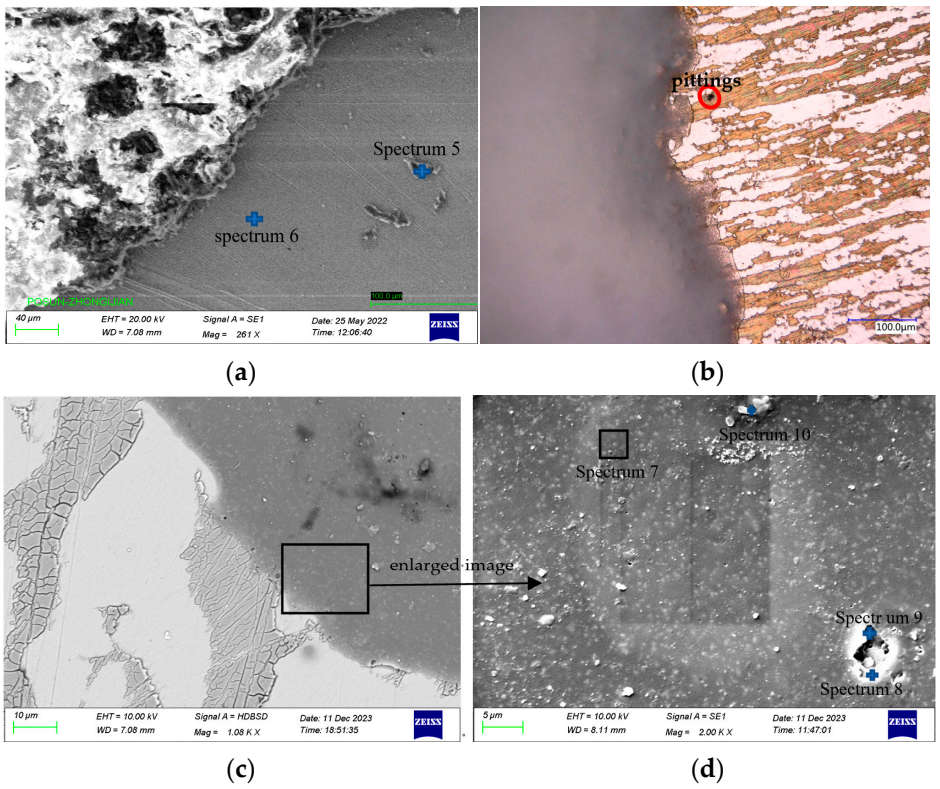

Figure 9. SEM image of coating damaged with φ1 mm circular hole. (**a**) HDR matrix corroded with coating damage. (**b**) Microstructure of coating damage after corrosion. (**c**) SEM of the connection between coating and HDR. (**d**) Enlarged image of coating.

Table 4. The result of EDS for different areas marked in Figure 9a (mass %).

Marked	Fe	Cr	Ni	Mn	Mo	Si	S	Cl	Na
Spectrum 5	51.9	19.6	4.9	1.5		0.4	0.6	9.3	11.9
Spectrum 6	66.2	23.2	8.0	1.7		0.4	0.5		

Table 5. The result of EDS for different areas marked in Figure 9d for coating (mass %).

Position	Markered	C	O	Si	Ti	Cl
Well-coated area	Spectrum 7	67.3	14.8	17.8		
Edges of coating hole edge	Spectrum 8	78.5	11.7		7.9	1.9
Coating holes	Spectrum 9	63.1	21.3	13.8	1.8	
White particulate matter	Spectrum 10	44.6	23.0		32.4	

3. Discussion

In the 3.5% NaCl solution, passivated HDR duplex stainless steel reacted with corrosive ions in the solution. The reaction formula was as follows:

$$\text{anode reaction: } Fe \rightarrow Fe^{2+} + 2e^{-}, \text{ and } Cr \rightarrow Cr^{3+} + 3e^{-} \quad (1)$$

$$\text{Cathode reaction: } O_2 + 2H_2O + 4e^{-} \rightarrow 4OH^{-} \quad (2)$$

After a short anode and cathode reaction, even if the matrix of metal coating damaged was gradually dissolved, the content of Fe^{2+} and Cr^{3+} was gradually increased, Passivation film was formed by Cr_2O_3,FeO,Fe_2O_3, and then corrosion products composed of $Fe(OH)_2$, Cr_2O_3, $Cr(OH)_3$, or $Fe(OH)_3$ were gradually formed as corrosion continued with coating damage [20–22]. The strip area of bare substrate was larger than 1 mm × 10 mm, and the impedance of the bare substrate was almost unchanged with the extension of the soaking time, which was quite different from metals such as carbon steel that are prone to corrosion. Compared with the coating damage area of 1 mm × 10 mm, the area of coating damage with a φ1 mm diameter round hole was smaller, but the HDR substrate impedance at the coating damage was increased. The impedance was 2 times that of the HDR uncoated protection at the beginning and increased to about 4 times that of the HDR uncoated protection after 15 days. The corrosion resistance was significantly enhanced with φ1 mm round hole coating damage, while the HDR substrate impedance with the 1 mm × 10 mm strip coating damage was not increased. The main reason for this is that while the coating was damaged at 1 mm × 10 mm, the system was equivalent to an open system, and the deposition effect caused by corrosion products was not obvious and could even be ignored. After solution immersion, the passivation film formed by the HDR matrix with 1 mm × 10 mm strip coating damage was almost the same as the whole sample without coating protection in the 3.5% NaCl solution. This was passive film work, showing that the impedance was close to that of the whole sample. The size of coating damage that reached a φ1 mm round hole was relatively small, and the deposition effect of corrosion products was obvious [23]. The dense passivation film and the newly formed corrosion product film made it difficult for oxygen outside the damaged coating to diffuse into the inside of the damaged coating, and the further occurrence of a corrosion reaction was terminated. The longer the time, the stronger the deposition effect caused by corrosion products. Therefore, the impedance value increased with the extension of the soaking time. The HDR impedance under the coating increased with the extension of the soaking time. With the extension of time, the corrosion products increase, and the formed corrosion product ions also enter the coating cavity to form a blockage, which enhances the isolation between the external corrosion medium and the substrate and enhances the corrosion resistance. In addition, as shown in Figure 9d, the self-made insulating coating has small pores, and the pores are

all contracted. Even if the pores are formed, they are filled with fillers such as TiO_2 and mica. Such fillers could enhance the shielding property of the coating and shield water and oxidation outside the substrate. The improved corrosion resistance of the substrate material [24] might also be due to the reported complex reaction between Fe ions and groups in the coating that improved the corrosion resistance of the substrate [25,26]. The ferritic structure is the preferred pitting corrosion in coating damage, which indicates that the ferrite of HDR duplex stainless steel is a weak phase in a 3.5% NaCl solution and easily corrodes [27,28]. At the same time, Cl ion adsorption [29–31] and S element inclusions [32] are the main factors causing the corrosion of stainless steel, which may be the main reasons for the preferential corrosion of the HDR ferrite structure.

4. Conclusions

HDR duplex stainless steel was protected by a self-made coating, the impedance was greatly improved, and the corrosion resistance was further improved. Even if the coating was damaged, it could achieve a better protection effect over 15 days and had the following characteristics:

(1) HDR was not protected by a coating or 1 mm × 10 mm strip coating damage. It was regarded as an open system. The LEIS impedance of the exposed metal matrix was stable, and the corrosion resistance was similar. However, the area of coating damaged was reduced to φ1 mm; with the extension of soaking time, the LEIS impedance of the exposed HDR matrix was 4 times than that of the bare HDR matrix without coating protection after 15 days, and the cumulative effect of corrosion products was obvious, which effectively promoted HDR corrosion resistance in the exposed areas after coating damage.

(2) The coating had a better protective effect on HDR duplex stainless steel. For the thinner coating with 1 mm × 10 mm strip coating damage, compared to that of φ1 mm round coating damage, the LEIS impedance reached a stable state faster. However, the thicker the coating, the greater the LEIS impedance and the better the corrosion protection of the coating.

(3) When the HDR duplex stainless steel surface coating was damaged, the LEIS impedance gradually increased along with the coating damage to the coating, and the further away from the coating damaged, the greater the increase in impedance, and the coating protection effect was obvious. HDR corrosion occurs preferentially on the ferrite structure after the coating is damaged, which is related to the weak phase of the structure and Cl^- adsorption.

Author Contributions: Methodology and supervision, Z.L.; formal analysis, X.L.; investigation, X.W.; data curation, J.C.; writing—original draft preparation, Y.L.; project administration, Z.Z. All authors have read and agreed to the published version of the manuscript.

Funding: This research received no external funding.

Institutional Review Board Statement: Not applicable.

Informed Consent Statement: Not applicable.

Data Availability Statement: The research data is all in the article.

Conflicts of Interest: The authors declare no conflict of interest.

References

1. AI, J.; Hu, Y.; Wang, H.; Liu, X. Research Progress on Corrosion of Duplex Stainless Steel and Its Welded Joint. *Surf. Technol.* **2022**, *51*, 77–91.
2. Yao, J. *The Microeletrochemical Behavior and the Stability of Passive Film on 2205 Duplex Stainless Steel*; University of Science and Technology Beijing: Beijing, China, 2019; pp. 53–80.

3. Wang, S.; Hu, Y.; Fang, K.; Zhang, W.; Wang, X. Effect of surface machining on the corrosion behaviour of 316 austenitic stainless steel in simulated PWR water. *Corros. Sci.* **2017**, *126*, 104–120. [CrossRef]
4. Zhang, P.; Xu, D.; Li, Y.; Yang, K.; Gu, T. Electron mediators accelerate the microbiologically influenced corrosion of 304 stainless steel by the Desulfovibrio vulgaris biofilm. *Bioelectrochemistry* **2015**, *101*, 14–21. [CrossRef]
5. Gao, Y.; Ren, S.; Liu, C.; Wu, X. Application of Micro Zone Electrochemical Technology in Corrosion and Assessment on the Coating Steel Structural. *J. Ningbo Univ. Technol.* **2021**, *33*, 13–20.
6. Zhang, H.; Ye, W.; Sun, B.; Huang, L. Corrosion and prevention of Duplex stainless steel in seawater pipline. *Corros. Prot.* **2013**, *34*, 45–48.
7. Lin, Y.; Wang, X.; Li, Z.; Zhang, X.; Wang, W. Effect of axial and radial micro-structure difference on corrosion resistance of HDR duplex stainless steel tubes. *J. Nav. Univ. Eng.* **2023**, *35*, 94–100.
8. Wang, J.; Qiu, X. Failure behavior of iron red epoxy primer in seawater by LEIS and EIS. *Mater. Prot.* **2016**, *49*, 23–25.
9. Huang, B.; Tang, B.; Feng, Y.; Wu, T.; Zeng, X.; Zhong, J.; Fu, X.; Huang, X.; Zhong, S. Analysis of pipeline stray current interference and corrosion protection coating damage. *NDT* **2023**, *45*, 1–6.
10. Zhang, R.; Xu, A.; Zhang, Z. Corrosion Behavior of Grey Organic Composite Coating for Vehicles at Different Damage Degree. *J. Mil. Transp. Univ.* **2017**, *19*, 92–95.
11. Wang, H.; Lian, B.; Wang, W.; Ma, S. Study on Synergic Protection Effect of Coating and Cathodic Protection for Three-Phase Separator. *Coat. Ang Prot.* **2023**, *44*, 54–61.
12. Balusamy, T.; Nishimura, T. In-Situ Monitoring of Local Corrosion Process of Scratched Epoxy Coated Carbon Steel in Simulated Pore Solution Containing Varying percentage of Chloride ions by Localized Electrochemical Impedance Spectroscopy. *Electrochim. Acta* **2016**, 305–313. [CrossRef]
13. Gao, J.; Qian, H.; Sun, X.; Guo, W.; Li, X. Effect of seawater pressure on protection properties of epoxy coating used in deep sea. *CIESC J.* **2015**, *66*, 4572–4577.
14. Kovačina, J.; Jegdić, B.; Radojković, B.; Marunkić, D.; Stevanović, S.; Simović, A. Influence of microstructure and roughness level on corrosion resistance of the austenitic stainless steel welded joint. *Mater. Corros.* **2021**, *72*, 1–17. [CrossRef]
15. Feng, X.; Zhang, L.; Zhang, J.; Lu, X.; Xu, Y.; Zhang, X.; Shi, R.; Chen, D. Effect of Aluminum Tri-polyphosphate on Corrosion Behavior of Reinforcing Steel in Seawater Prepared Coral Concrete. *J. Wuhan Univ. Technol.-Mater.* **2019**, *34*, 906–913. [CrossRef]
16. Wang, S.; Gu, Y.; Geng, Y.; Liang, J.; Zhao, J.; Kang, J. Investigating local corrosion behavior and mechanism of MAO coated 7075 aluminum alloy. *J. Alloys Compd.* **2020**, *826*, 1–13. [CrossRef]
17. Nardeli, J.V.; Fugivara, C.S.; Taryba, M.; Montemor, M.F.; Benedetti, A.V. Biobased self-healing polyurethane coating with Zn micro-flakes for corrosion protection of AA7475. *Chem. Eng. J.* **2020**, *404*, 126478–126492. [CrossRef]
18. Zeng, H.; Yang, Y.; Zeng, M.; Li, M. Effect of dissolved oxygen on electrochemical corrosion behavior of 2205 duplex stainless steel in hot concentrated seawater. *J. Mater. Sci. Technol.* **2021**, *66*, 177–185. [CrossRef]
19. Leng, A.; Streckel, H.; Stratmann, M. The delamination of polymeric coatings from steel. Part 2: First stage of delamination, effect of type and concentration of cations on delamination, chemical analysis of the interface. *Corros. Sci.* **1998**, *41*, 579–597. [CrossRef]
20. Duan, T.; Xu, L.; Ding, K.; Peng, W.; Hou, J.; Guo, W.; Cheng, W. Corrosion behaviour investigation of 460 low alloy steels exposed in the natural deep-sea environment. *Corros. Eng. Sci. Technol.* **2019**, *54*, 485–492. [CrossRef]
21. Duan, T.; Peng, W.; Ding, K.; Guo, W.; Hou, J.; Cheng, W.; Liu, S.; Xu, L. Long-term field exposure corrosion behavior investigation of 316L stainless steel in the deep sea environment. *Ocean. Eng.* **2019**, *189*, 106405. [CrossRef]
22. Wang, M.; Zeng, S.; Zhang, H.; Zhu, M.; Lei, C.; Li, B. Corrosion behaviors of 316 stainless steel and Inconel 625 alloy in chloride molten salts for solar energy storage. *High Temp. Mater. Process.* **2020**, *39*, 340–350. [CrossRef]
23. Liu, P.; Zhang, Q.; Li, X.; Hu, J.; Cao, F. Insight into the triggering effect of (Al, Mg, Ca, Mn)-oxy-sulfide inclusions on localized corrosion of weathering steel. *J. Mater. Sci. Technol.* **2021**, *64*, 99–113. [CrossRef]
24. Zhang, S.; Wang, P.; Zhu, F.X.; Shi, M.H. Effect of Nickel Content on Mechanical Property and Microstructure for Sulfide Stress Corrosion High-Strength Steel. *Mater. Sci. Forum* **2018**, *939*, 16–22. [CrossRef]
25. Lu, X.; Zuo, Y.; Zhao, X.; Tang, Y. The influence of aluminum tri-polyphosphate on the protective behavior of Mg-rich epoxy coating on AZ91D magnesium alloy. *Electrochim. Acta* **2013**, *93*, 53–64. [CrossRef]
26. Cheng, L.; Liu, C.; Wu, H.; Zhao, H.; Mao, F.; Wang, L. Mussel-inspired delivery system for enhancing self-healing property of epoxy coatings. *J. Mater. Sci. Technol.* **2021**, *80*, 36–49. [CrossRef]
27. Ha, H.Y.; Lee, T.H.; Lee, C.G.; Yoon, H. Understanding the relation between pitting corrosion resistance and phase fraction of S32101 duplex stainless steel. *Corros. Sci.* **2019**, *149*, 226–235. [CrossRef]
28. Zeng, H.; Yang, Y.; Liu, L.; Li, M. Pitting and crevice corrosion evolution characteristics of 2205 duplex stainless steel in hot concentrated seawater. *J. Solid State Electrochem.* **2021**, *25*, 1555–1565. [CrossRef]
29. Wang, J.; Shi, W.; Xiang, S.; Ballinger, R.G. Study of the corrosion behaviour of sensitized 904L austenitic stainless steel in Cl^- solution. *Corros. Sci.* **2021**, *181*, 109234–109241. [CrossRef]
30. Li, J.; Zhong, X.; Wang, T.; Shang, T.; Hu, J.; Zhang, Z.; Zeng, D.; Hou, D.; Shi, T. Synergistic effect of erosion and hydrogen on properties of passive film on 2205 duplex stainless steel. *J. Mater. Sci. Technol.* **2021**, *67*, 1–10. [CrossRef]

31. Li, L.; Yan, J.; Xiao, J.; Sun, L.; Fan, H.; Wang, J. A comparative study of corrosion behavior of S-phase with AISI 304 austenitic stainless steel in $H_2S/CO_2/Cl^-$ media. *Corros. Sci.* **2021**, *187*, 109472–109482. [CrossRef]
32. Nishimoto, M.; Muto, I.; Sugawara, Y.; Hara, N. Cerium addition to CaS inclusions in stainless steel: Insolubilizing water-soluble inclusions and improving pitting corrosion resistance. *Corros. Sci.* **2021**, *180*, 109222–109230. [CrossRef]

Disclaimer/Publisher's Note: The statements, opinions and data contained in all publications are solely those of the individual author(s) and contributor(s) and not of MDPI and/or the editor(s). MDPI and/or the editor(s) disclaim responsibility for any injury to people or property resulting from any ideas, methods, instructions or products referred to in the content.